Hindawi
Advances in Polymer Technology
Volume 2021, Article ID 2966920, 12 pages
https://doi.org/10.1155/2021/2966920

Research Article

Continuous Differential Microemulsion Polymerization to Prepare Nanosized Polymer Latices in Microreactors

Min Qiu,[1] **Liang Xiang**,[1] **Minjing Shang**,[1] **and Yuanhai Su**[1,2]

[1]*Department of Chemical Engineering, School of Chemistry and Chemical Engineering, Shanghai Jiao Tong University, Shanghai 200240, China*
[2]*Key Laboratory of Thin Film and Microfabrication (Ministry of Education), Shanghai Jiao Tong University, Shanghai 200240, China*

Correspondence should be addressed to Yuanhai Su; y.su@sjtu.edu.cn

Received 9 September 2021; Accepted 9 November 2021; Published 24 November 2021

Academic Editor: Kai Guo

Microreactors are a promising platform for continuous synthesis of polymer latices when combined with emulsion polymerization. However, this application has long been haunted by fouling and clogging problems. In this work, we proposed the strategy of conducting differential microemulsion polymerization in microreactors within a biphasic slug flow and achieved rapid and stable preparation of nanosized PMMA latices (polymeric content as high as 15.7% with average particle size smaller than 20 nm). We started by exploring the temperature thresholds with thermal and redox initiation, the effect of initiator concentration, and the kinetic characteristics of microemulsion polymerization at different temperatures. Then, as for the differential microemulsion polymerization, extensive investigation was made into the effects of the volumetric flow ratio, the prepolymerization time, the initiator concentration, and the solid content of the initial microemulsion. Finally, we compared the differential microemulsion polymerization with the soap-free emulsion polymerization in the slug flow. The striking advantages in the polymerization rate, the average particle diameter, and the size distribution reflected higher density of particle nuclei, larger specific surface area of particles, and the pivotal effect of the persistent particle nucleation in the microemulsion polymerization.

1. Introduction

Emulsion polymerization is a representative heterogeneous polymerization of great importance in both academia and industry. Typical emulsion polymerization takes place in an oil-in-water (O/W) emulsion, in which droplets of monomer are dispersed by emulsification and the solution of initiator serves as the continuous phase. Not only does the compartmentalization of polymerization process in emulsion make it possible to produce polymers of high molar mass without compromising high rate of polymerization, but it also improves heat removal and mitigates the viscosity problem compared with bulk polymerization [1, 2]. Using water as the continuous phase, emulsion polymerization is widely adopted as an environmentally friendly process to polymerize various relatively hydrophobic monomers such as styrene, acrylonitrile, acrylate ester, methacrylate ester, vinyl acetate, and vinyl chloride [3, 4] The products can be used either in a direct way as commercial latices (such as paints, adhesives, and coatings) or isolated by coagulation or drying to form rubbers and thermoplastics [2].

Emulsion polymerization and its derivative methods, i.e., miniemulsion and microemulsion polymerization, are now important ways for the preparation of nanoparticles. The monomer droplets in conventional emulsion, miniemulsion, and microemulsion are of 1-100 μm, 50-1000 nm, and 10-100 nm, respectively, therefore enabling the synthesis of polymer particles with different sizes and morphologies [1]. Microemulsion polymerization is commonly regarded as a suitable technique to produce nanosized polymer latices. However, a large amount of surfactant along with a relatively low amount of monomer is required to form this thermodynamically stable system, which demands expensive postproduction processing to concentrate the products [5].

Differential microemulsion polymerization, involving continuous dropwise addition of monomer into a prepolymerized microemulsion system, has been hitherto reported to overcome this problem. Aside from increasing the solid content of the product to a certain extent, this method also avoids risking the capability to produce rather small particles. Applying this method, He et al. [6] synthesized a PMMA latex with a particle size of 13-16 nm and a solid content of 13.7 wt.%, whereas Wang et al. [7] took a step further and prepared a PMMA latex of 2-5 nm with a comparable solid content.

The past few decades have witnessed the rapid development of microreactor technology and its application in polymerization. Renowned as not only a promising platform of process intensification but also a competitive alternative for chemical production, microreactors offer outstanding features absent in conventional batch reactors, including their excellent mixing efficiency, enhanced mass and heat transfer [8], improved safety [9], and precise control over process parameters [10, 11]. These merits endow microreactors unprecedented advantages to handle highly exothermal reactions like polymerization.

Homogeneous polymerization has prospered in the employment of microreactors. Various kinds of polymerization were conducted including free radical polymerization [12], RAFT polymerization [13], organocatalyzed ATRP [14], cationic polymerization [15], anionic polymerization [16], and ring-opening polymerization [17]. Moreover, microreactors are ready to scale up the homogeneous polymerization in a numbering-up strategy [18, 19]. If assembled in a cascade fashion, microreactors also enable the synthesis of polymers with complex structures such as block polymers [20] and star polymers [21, 22].

Although heterogeneous polymerization is not as common as homogenous polymerization in microreactors, recent research has demonstrated that polymerization taking place in immiscible phases benefits a lot from the high specific surface area and the internal recirculation inside the slugs. Song et al. [23] performed the chemical oxidative polymerization of aniline within a slug flow regime and found that microreactors can significantly improve the mass transfer for the polymerization process. Watanabe et al. [24] proposed a similar way to implement soap-free emulsion polymerization of MMA and prepared PMMA with weight-average molecular weight as high as 1500 kg/mol within 20 min in the slug flow. Apart from utilizing slug flow for mass transfer intensification, emulsion polymerization, as an innate heterogeneous method of polymerization, has also been employed directly in microreactors. Lobry et al. [25, 26] realized the continuous synthesis of poly(acrylate) particles through miniemulsion photopolymerization in microreactors at room temperature and pointed out that the colloidal stability of the miniemulsion is crucial for avoiding clogging and fouling. Liu et al. [27] exploited the mixed emulsifier TX-100/SDBS to improve the stability of the preemulsion and achieved rapid preparation of polystyrene nanoparticles through continuous emulsion polymerization. Besides the emulsion stability, there are many other factors that lead to clogging in tubular reactors, such as the adhesional wetting of monomers, solid content, and tubing diameter [28, 29]

The aim of this paper is to achieve stable and rapid synthesis of polymer latices through emulsion polymerization in capillary microreactors. Our strategy is to conduct the differential microemulsion polymerization through the gradual diffusion of monomer in a biphasic slug flow, which, to the best of our knowledge, has not been reported in literature. This method is based on two fundamental theories. That is, the microemulsion is thermodynamically stable which grants the stability of the aqueous phase. Meanwhile, the organic phase can wet the wall of the capillary microreactor and form an organic liquid film, thus preventing monomer from adhering to the wall and fouling. In this work, we first assessed the temperature thresholds with different initiation systems and the effect of the initiator concentration on the MMA conversion and conducted the kinetic modeling in the polymerization of the initial microemulsion. Then, we investigated extensively the effects of the volumetric flow ratio, the prepolymerization time, the initiator concentration, and the solid content in the initial microemulsion on the final polymer latices. Lastly, a comparison between the differential microemulsion polymerization and the soap-free emulsion polymerization was performed from aspects of conversion versus residence time profile, number-average particle size, and the evolution of size distribution.

2. Experimental

2.1. Materials and Apparatus. Methyl methacrylate (MMA) (AR, 99.0 wt.%), acquired from Aladdin Biochemical Technology Co., Ltd. (Shanghai, China), was washed with sodium hydroxide aqueous solution for inhibitor removal and dehydrated with activated 4A zeolite. Ammonium persulfate (APS) (AR, 98.0 wt.%) and sodium dodecyl sulfate (SDS) (AR, 88.0%) from Titan Scientific Co., Ltd. (Shanghai, China) served, respectively, as initiator and emulsifier without further purification. N,N,N′,N′-Tetramethylethylenediamine (TMEDA) (AR, 99%) from InnoChem Science & Technology Co., Ltd. (Beijing, China), was used to pair with APS to form the redox initiation system. Apart from deionized water, dodecane (AR) was used as the solvent in the organic phase.

Polyether ether ketone (PEEK) T-micromixers, unions, luer adapters, and perfluoroalkoxy (PFA) capillaries were purchased from Valco Instruments Co. Inc. (USA). Capillaries involved in this work were of the same inner diameter (1.0 mm) and the same outer diameter (1/16 inch). Syringe pumps were purchased from New Era Pump System, Inc. (USA).

2.2. Continuous Polymerization of the Initial Microemulsion. The preparation of the initial microemulsion was done in two steps. First, the aqueous mixture including 2.5 wt.% SDS and 2.5 wt.% MMA was stirred at 500 rpm for more than 1 hour. We could observe that the previously translucent mixture turned transparent when the thermodynamic equilibrium was achieved, which usually takes only a few minutes. Second, a specific amount of initiator was dissolved

with stirred microemulsion in the volumetric flask to adjust its concentration.

The initial microemulsion was then continuously injected into a capillary microreactor by a syringe pump (as depicted in the upper-left corner of Figure 1). For the redox-initiated microemulsion polymerization, reductive and oxidative initiators were dissolved and injected separately. The conversion of MMA was measured gravimetrically.

2.3. Continuous Differential Microemulsion Polymerization in Biphasic Slug Flow. Figure 1 displays the entire setup of the continuous differential microemulsion polymerization. We introduced the organic phase (MMA/dodecane) at the end of the microemulsion prepolymerization by a second syringe pump to feed more MMA into the system. A typical slug flow regime was observed owing to the immiscibility of the solvents under all involved operating conditions (specified operating parameters are listed in Table 1). The flow was eventually immersed in an ice-water bath to quench the polymerization. Furthermore, a third pump would be integrated to adjust the conditions (e.g., the solid content of the initial microemulsion) when needed. In this manner, we realized the continuous differential microemulsion polymerization of MMA in the capillary microreactor. It should be noted that two periods of time were involved in this method, namely, one for the microemulsion prepolymerization and the other for the differential microemulsion polymerization. They are referred to as the prepolymerization time (t_1) and the residence time (t_2), respectively, in the following sections about the differential microemulsion polymerization. All the experiments are repeated at least three times.

2.4. Characterization of the Final Polymer Latices. The monomer conversion was calculated by tracking the residual MMA concentration through gas chromatography (GC, Agilent 7890B equipped with a flame ionization detector, USA). That is, 200 μL sample of the organic phase was diluted with acetone (1 : 10 *v*/*v*), and then, the mixture was injected into the GC system by an autosampler. The dodecane served as internal standard to calibrate the concentration of MMA.

After being precipitated with ethanol, washed with warm water, and centrifuged for multiple times, the products were dried under vacuum and sent to characterize their molar mass properties through gel permeation chromatography (GPC, Tosoh EcoSEC 8320, Japan) at 40°C with tetrahydrofuran (THF) as the mobile phase.

The number-average size and the size distribution of the polymer latices were measured by dynamic light scattering (DLS, Malvern Zetasizer Nano ZS90, UK) at 25°C. The morphologies of the dried polymer latices were captured by a scanning electron microscope (SEM, FEI Nova NanoSEM 450, USA) after gold sputtering.

3. Results and Discussion

3.1. Polymerization of the Initial Microemulsion

3.1.1. Temperature Thresholds with Different Initiators. Initiation plays a crucial role in free radical polymerization. For emulsion polymerization with aqueous continuous phase, thermal initiators are commonly adopted, and the process is often conducted at 75-90°C to maximize the production rate. In recent years, redox initiator systems are reported to expand the envelope of operating temperature in emulsion polymerization [30]. At the stage of initial microemulsion polymerization, APS was used solely as a thermal initiator and also combined with TMEDA to form a redox initiation system. The comparison of these two initiation methods was carried out with concentrations of the initiators set to 5 mM and residence time set to 10 min. We varied the operating temperature to assess the performance of initiation. As shown in Figure 2, both initiation methods would give a higher rate of polymerization with the operating temperature increasing. Nevertheless, they differed a lot in the temperature thresholds. At 45°C, when the redox initiation system already showed high conversion of monomer, the polymerization through thermal initiation only brought about little conversion. Thermal initiation did not provide considerable monomer conversion until the temperature was above 70°C. Although it is evident that the redox initiation prevailed in the low-temperature region, instant precipitation of the products was necessary in order to determine the monomer conversion precisely because the ice-water bath was often inadequate to quench the redox-initiated polymerization. Furthermore, the reductive and the oxidative parts of initiator system have to be dissolved in separate premicroemulsion, which would complicate the operation especially if various conditions were taken into consideration. Therefore, to mitigate the operational complexity, we performed the experiments through thermal initiation in the following sections. Since the discrepancy between these two methods lies in mainly the initiation efficiency, the ensuing discussions about thermally initiated polymerization should be credible in redox initiation system once given comparable conditions.

3.1.2. Effect of the Initiator Concentration on the Conversion of MMA. The initiator concentration is also the key to effective initiation of the polymerization. We conducted the microemulsion polymerization at 70°C for 5 min and 10 min with the concentration of APS ranging from 2.5 to 10 mM. It can be inferred from Figure 3 that higher concentration of the initiator is essential to a rapid polymerization. When the concentration of APS reached 10 mM, the conversion at 5 min was very close to that at 10 min. However, there is also a tendency that the slope of conversion climbing is getting flatter as the concentration of APS increases, indicating that the marginal effect of raising the initiator dosage tends to ebb.

3.1.3. Kinetic Study of Microemulsion Polymerization in Flow. Before stepping forward to the continuous differential microemulsion, it is necessary to single out the intrinsic kinetics of microemulsion polymerization here to avoid the effect of interphasic mass transfer.

Conventional emulsion polymerization comprises of the particle nucleation (interval I) and the particle growth (intervals II and III).[1, 2, 4]. Owing to the fact that a relatively large amount of surfactant is used in microemulsion

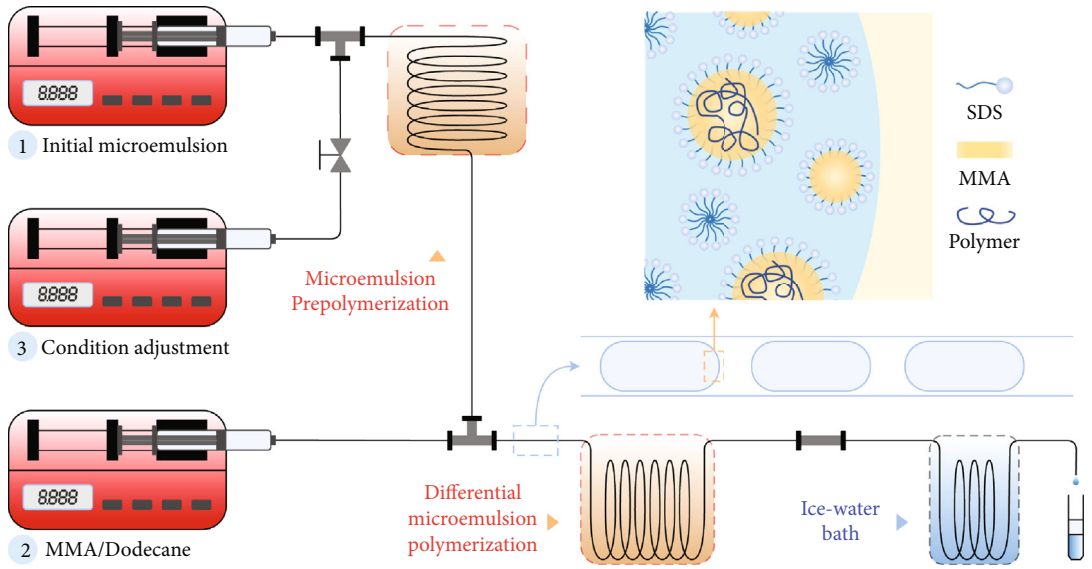

Figure 1: Schematic overview of the differential microemulsion polymerization carried out in a biphasic slug flow.

Table 1: Specified parameters of continuous differential microemulsion polymerization.

Compositions	Initial microemulsion Organic phase	MMA/SDS = 1 : 1 wt./wt., APS, water MMA/dodecane = 1 : 4 *v*/*v*
Operating conditions	Flow ratio	W : O = 1 : 1 – 2 : 1, Q_{total} = 0.125 mL/min
	Temperature	70–85°C
	Prepolymerization time	0–20 min
	Residence time	4–40 min

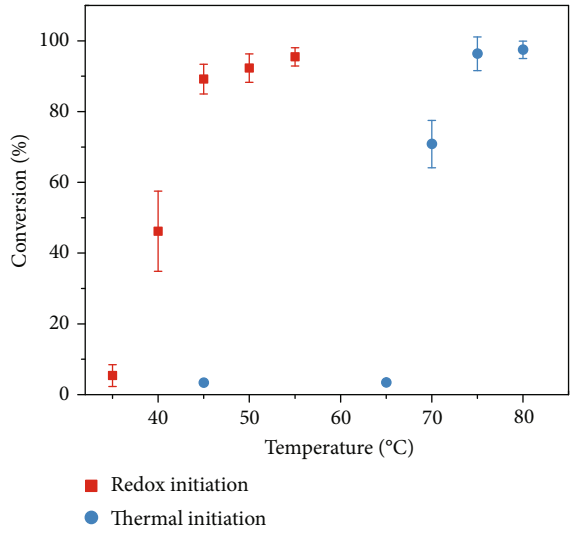

Figure 2: Temperature thresholds with different initiation systems in the capillary microreactor (t = 10 min and the concentration of the initiator involved was 5 mM).

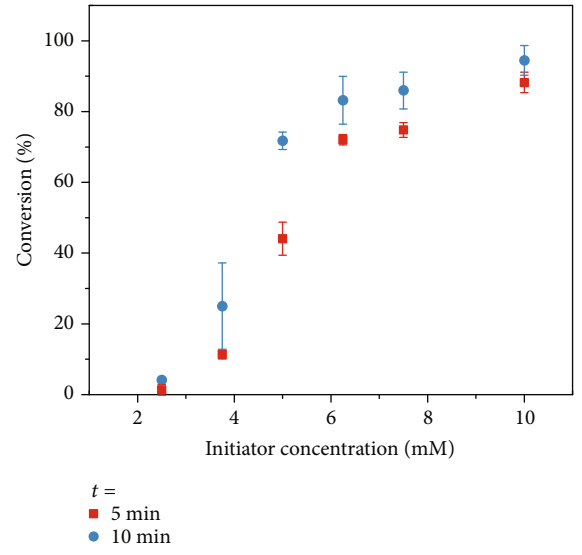

Figure 3: Effect of the initiator concentration on the MMA conversion at 70°C.

polymerization, the particle nucleation occurs over most of the process. Therefore, interval II, which features an approximately constant rate of polymerization, is absent in the microemulsion polymerization [1]. The kinetic model proposed by Morgan et al. is one of the most extensively adopted models [31, 32]. The Morgan model is usually deduced as follows.

The fundamental governing equation for microemulsion polymerization considers the rate of polymerization first order in the concentrations of both monomer and propagating radicals:

$$\frac{\mathrm{d}X}{\mathrm{d}t} = \frac{k_p C_M N^*}{M_0}, \tag{1}$$

where X is the fractional conversion, M_0 is the initial monomer concentration in the microemulsion, C_M is the monomer concentration at the locus of polymerization, N^* is the concentration of radicals propagating in the particles, and k_p is the rate constant of propagation. Among these parameters, C_M and N^* change throughout the process. To determine these two parameters is of crucial importance.

Provided that the number of the micelles is much greater than that of the particles, it is rather rare for the radicals generated in the aqueous phase to enter a polymer particle bearing an active radical. Similarly, the chance of the radicals terminating in the aqueous phase is also negligible. As a result, the time dependence of N^* is roughly the decomposition of the initiators:

$$\frac{\mathrm{d}N^*}{\mathrm{d}t} = 2k_d f[I], \tag{2}$$

where one initiator is assumed to decompose into two radicals, k_d is the rate constant of dissociation, f is the initiation efficiency, and $[I]$ is the initiator concentration. On account of that the half-life of the initiator is significantly longer that the time of polymerization, one can further simplify the model by assuming that $[I]$ is constant.

Another prevalent postulate is that C_M varies linearly with the change of the conversion, namely,

$$C_M = C_0(1 - X), \tag{3}$$

where C_0 is the initial monomer concentration in the particles when sufficient polymers have formed to absorb all available monomer.

Substituting Equations (2) and (3) into Equation (1), we can get the conversion in the Morgen model as a function of time:

$$X = 1 - \exp\left(-\frac{k_p k_d C_0 f[\mathrm{I}]}{M_0} t^2\right). \tag{4}$$

With all the chemical parameters considered constant, Equation (4) can be simply expressed by grouping them into one single parameter A:

$$X = 1 - \exp\left(-At^2\right). \tag{5}$$

An interesting prediction contained in this model is that the rate of polymerization always reaches its maximum at a conversion of 0.39, independent of the parameters mentioned above.

Herein, we tracked the monomer conversion along the microemulsion in the capillary microreactor at different temperatures of 70, 75, and 80°C. Out of the simplification of the fitting process, Equation (5) can be converted into a linear model:

$$\sqrt{-\ln(1 - X)} = kt, \tag{6}$$

where k equals the square root of the kinetic parameter A.

The relationship between conversion and residence time is displayed in Figure 4. There was a twist when the polymerization proceeded to a certain extent at either temperature, indicating a rapid degradation of the polymerization rate. This phenomenon can be frequently found in relative research. Morgan et al. attributed it to the autoinhibition mechanism in persulfate-initiated systems which would depreciate the initiation efficiency [31]. Nevertheless, there is still recognizable linearity on either side of the twist. Therefore, the relationship between conversion and residence time was supplemented into a piecewise function:

$$\begin{cases} \sqrt{-\ln(1 - X)} = kt, & 0 \le t \le t_0, \\ \sqrt{-\ln(1 - X)} = k't + c, & t_0 < t, \end{cases}$$
$$k't + c = k'\left(t + t'\right), \tag{7}$$
$$t_0 = \frac{c}{k - k'},$$

where k' denotes the kinetic parameter in the second region, t' stands for the time deviation for the second region, t_0 is the time when the twist happens, and c equals the product of k' and t' to simplify the fitting process.

The fitting was done with the method of robust least squares in Python 3.8. The results are given in Table 2, and a graphic presentation is shown in Figure 4. This model fits well on both sides of the twist point. The rapid increment of k suggests that the polymerization rate rose significantly as the temperature increased. A higher operating temperature also postponed the degradation of the polymerization rate until the conversion of MMA exceeded approximately 90%.

We also compared the experimental data with the prediction made from the Morgan model and the piecewise model developed here (see Figure 5). The Morgan model shows the tendency in an ideal microemulsion polymerization, while the piecewise one is close to the real situation in our experiments and reflects the degradation of the polymerization rate in the end. The agreement between the data and the model confirms the fact that unlike typical emulsion polymerization, there is no period of constant polymerization rate and particle nucleation happens continuously in the microemulsion polymerization. This mechanism of microemulsion polymerization, as readers will find in the following sections, has profound influence on the continuous differential microemulsion polymerization.

3.2. Differential Microemulsion Polymerization in Biphasic Flow

3.2.1. Effect of the Volumetric Flow Ratio on the Monomer Conversion. In conventional batch reactors, the differential microemulsion polymerization usually utilizes the dropwise addition of monomer to increase the molar ratio of polymer to surfactant. Unlike reaction tanks for differential

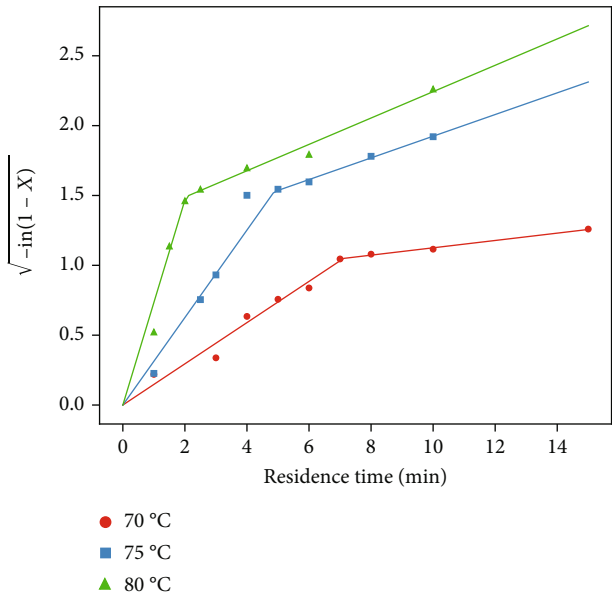

Figure 4: Piecewise linear fitting at different temperatures.

Table 2: The regression coefficients and r-square statistics.

Temperatures (°C)	First region	Second region		r^2
	k	k'	t'	
70	0.1475	0.0263	32.80	0.9796
75	0.3131	0.0766	14.99	0.9712
80	0.7336	0.0944	13.76	0.9743

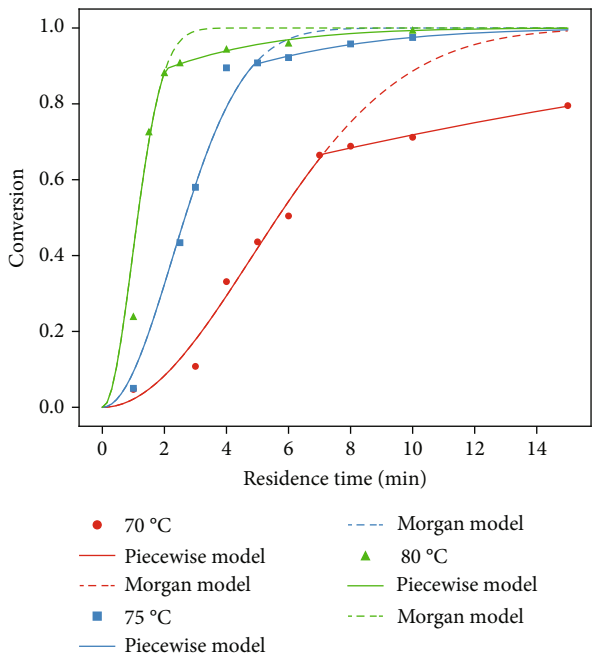

Figure 5: Comparison of the experimental data and the simulated data.

microemulsion polymerization that require vigorous stirring and precise control of dropping pace, the continuous addition of monomer is realized by means of the gradual transfer of monomer from the continuous phase to the dispersed phase in a biphasic flow system. As reported in relevant research [23, 33], the mass transfer performance of microreactors is reported to be strongly affected by the overall Reynolds number and the volumetric flow ratio of the aqueous phase to the organic phase.

For the immiscible liquid-liquid biphasic system, the overall Reynolds number (Re_M) can be calculated through the pseudohomogeneous model [34]:

$$\begin{aligned}
\mathrm{Re}_M &= \frac{\rho_M \cdot d_i \cdot u_M}{\mu_M}, \\
u_M &= \frac{4}{\pi} \cdot \frac{Q_{aq} + Q_{or}}{d_i^2}, \\
\rho_M &= \left(\frac{\varphi_{or}}{\rho_{or}} + \frac{1-\varphi_{or}}{\rho_{aq}}\right)^{-1}, \\
\mu_M &= \left(\frac{\varphi_{or}}{\mu_{or}} + \frac{1-\varphi_{or}}{\mu_{aq}}\right)^{-1}, \\
\varphi_{or} &= \frac{Q_{or}}{Q_{aq} + Q_{or}},
\end{aligned} \tag{8}$$

where d_i is the inner diameter of the microchannel, ρ_{or}, ρ_{aq}, μ_{or}, μ_{aq}, Q_{or}, and Q_{aq} represent the density, the viscosity, and the volumetric flow rate of the aqueous phase and the organic phase, respectively.

In this section, we performed the polymerization with a constant overall volumetric flow rate of 0.125 mL/min in a capillary microreactor with 1 mm inner diameter so that the overall velocity was maintained at 0.265 cm/s. Based on the physical properties given in Table 3, when we increased the volumetric flow ratio from 1 to 2, Re_M only underwent gentle change from 2.38 to 2.56. Therefore, the dominant factor here was the volumetric flow ratio.

The comparison was made at four incremental temperatures, and the results are given in Figure 6. As the flow ratio of the aqueous phase to the organic phase increased from 1.0 to 2.0, there was significant improvement in the conversion at 75 and 80°C. At 70 or 85°C, the polymerization rate was either too low or too high, which mitigated the distinction among different flow ratios. This observation is in good agreement with that of Song et al. [23] when they increased the flow ratio from 0.5 to 3.0 and obtained an increase of PANI yield from 20% to 80%. This intensification effect of a higher flow ratio was mainly attributed to the expansion of the specific surface area, which accelerates the diffusion of the monomer from the organic phase to the reactive aqueous phase. In addition, at 85°C with the flow ratio of 1.0, the polymeric content of the final latex could reach 15.7% after 20 min, which is comparable to the latices prepared from conventional flasks in He et al.'s and Wang et al.'s work [6, 7]. This observation substantiates the capability of

Table 3: Physical properties of the involved fluids at 25°C.

Substances	Viscosity (mPa·s)	Density (kg/m^3)
Water [35]	0.890	997
MMA [36]	0.584	937.8
Dodecane [37]	1.36	773.9

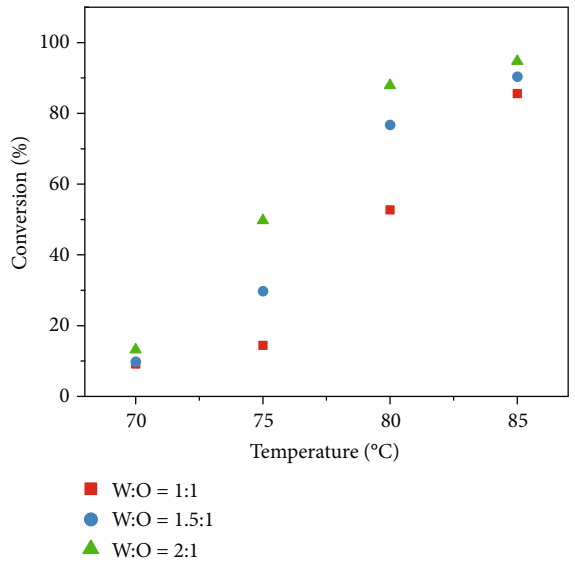

Figure 6: Effect of the volumetric flow ratio on the monomer conversion at different temperatures ($t_1 = t_2 = 20$ min, and the concentration of APS was 5 mM).

continuous-flow microreactors as a feasible and sufficient way of latex production.

3.2.2. Effect of the Prepolymerization Time on the Monomer Conversion. As mentioned in the kinetic study of the microemulsion polymerization, the microemulsion system will eventually change from a monomer-abundant state into a monomer-starved system. It should be taken into consideration how the state of the prepolymerized microemulsion is when contacting with the organic phase. We varied the prepolymerization time from 0 to 20 min and conducted the differential polymerization at 75 and 80°C for 20 min. From Figure 7, it can be seen that the conversion of MMA rose steadily as the prepolymerization time increased. The elongation of the monomer-starved state seemed to help boost the polymerization rate in the differential polymerization stage, which might be attributed to the high residual concentration of free radicals when the system was short of monomer.

3.2.3. Effect of the Initiator Concentration on the Monomer Conversion and the Molar Mass Properties. The initiator concentration has a great impact on not only the effective initiation of polymerization but also the final products. For emulsion polymerization, the degree of polymerization ($\bar{X}_n$) can be given by Equation (9) [1]. The degree of polymerization varies with the rate of polymerization (r_p), the rate of

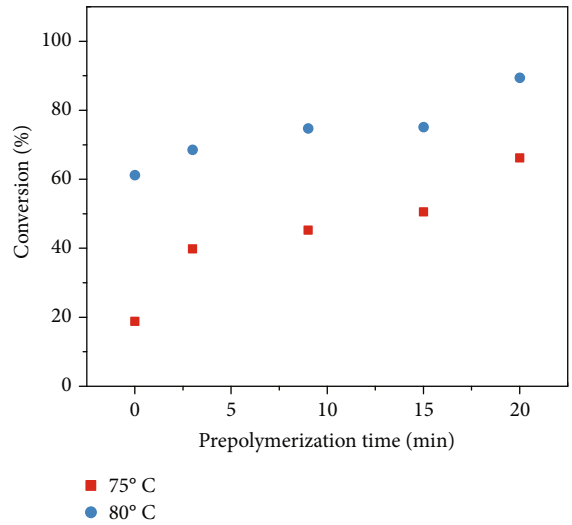

Figure 7: Effect of the prepolymerization time on the monomer conversion at 75 and 80°C (W : O = 2 : 1, $t_2 = 20$ min, and the concentration of APS was 5 mM).

initiation (r_i), and the rate of chain transfer (r_{tr}). If the rate of initiation is maintained, it is possible to increase the degree and rate of polymerization at the same time, which explains the aforementioned unique attribute of emulsion polymerization. Since the rate of polymerization is also affected by the initiator concentration, the impact of the initiator dosage on the degree of polymerization is indirect.

$$\bar{X}_n = \frac{r_p}{r_t + \sum r_{tr}}. \quad (9)$$

The effect of the APS concentration on the conversion of MMA and the molar mass of the polymer product is displayed in Figure 8. As the concentration of APS increased from 1.25 mM to 5 mM, the conversion of MMA soared and the molar mass dropped quickly, implying an increase in the rate of polymerization and a decrease in the degree of polymerization, respectively. The impact of the initiator concentration was no longer distinctive when we further increased the APS concentration. The conversion of MMA increased slightly as a residence time of 40 min was considerably adequate for the differential microemulsion polymerization with a high level of initiator concentration. The high polymerization rate seemed to offset the impact of the high initiator concentration on the degree of polymerization to some extent so that the molar mass of the products was still as high as 85 kg/mol when the APS concentration was 20 mM. The polydispersity of the products fluctuating from 3.1 to 4.2 implied a relatively wide distribution of molar mass. The relatively high polydispersity could be explained from two aspects as follows. Since the rate of initiation is low in free radical polymerization, the chain initiation occurs all along the process. Furthermore, a relatively wide distribution of polymerization time might result from the uneven diffusion of the monomer.

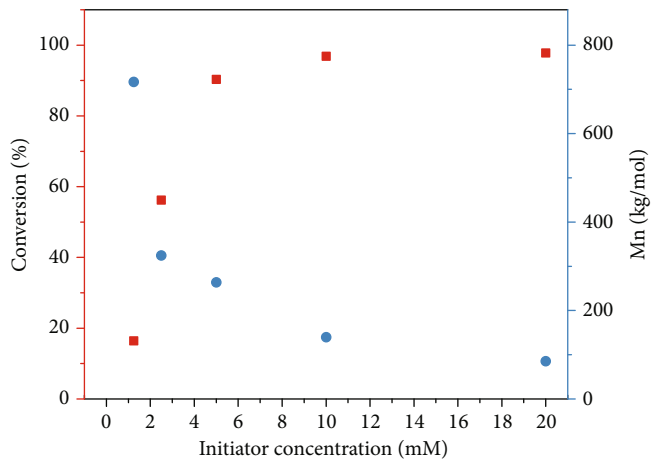

Figure 8: Effect of the initiator concentration on the monomer conversion and the number-average molecular weight (W : O = 1.5 : 1, T = 80°C, t_1 = 20 min, and t_2 = 40 min).

3.2.4. Effect of the Solid Content in the Initial Microemulsion on the Monomer Conversion. For microemulsion polymerization, the use of a great amount of surfactant is often a "necessary evil" to control the particle size, which may increase difficulty and cost for purification of polymer products. One preferable goal of differential microemulsion is to avoid the overdose of surfactant and increase the ratio of polymer to surfactant. In this work, the surfactant was only added at the very beginning in the initial microemulsion. Therefore, it is convenient for microreactors to adjust the solid contents of initial microemulsion by inline dilution with an aqueous solution of initiator. In Figure 9, we investigated the effect of the solid content in the initial microemulsion on the polymerization performance. For a residence time of 20 min, the conversion of MMA firstly increased rapidly with a higher solid content and then reached a plateau. When the residence time was elongated to 40 min, the difference in MMA conversion was negligible among the solid content ranging from 1.0% to 5.0%, indicating that the polymerization was near its completion. Although there did exist a trade-off between the high polymer proportion and the high polymerization rate, our experiments proved the possibility of preparing polymer latices with high polymer proportion in continuous-flow microreactor.

Note that when the solid content in the initial microemulsion was 0, the solution of initiator instead of the initial microemulsion was fed into the microreactor, and this process was the soap-free emulsion polymerization just as Watanabe et al. [24] did. There was, however, a conspicuous difference among the polymer latices synthesized. The polymer latex prepared in soap-free emulsion polymerization was an opaque milky liquid; by contrast, polymer latices by the other method were transparent bluish liquids (see Figure S1 in Supporting Information). This phenomenon indicates that there must be some intrinsic distinction between these two methods. A more detailed comparison between these two methods was arranged in the next section.

3.3. Comparison between Differential Microemulsion and Soap-Free Emulsion Polymerization. As discussed in previous sections, microemulsion polymerization differs from typical emulsion polymerization in the particle growth mechanism. To evaluate the effect of this difference on the polymerization process and final products, we made a comparison between differential microemulsion and soap-free emulsion polymerization in the continuous biphasic slug flow by tracking the chronological conversion of MMA, the average particle diameter, and the particle size distribution in both methods. The polymerization process of either method was conducted after a twenty-minute prepolymerization/preheating of the initial microemulsion/solution.

From Figure 10, the differential microemulsion polymerization of MMA showed a much higher polymerization rate than the soap-free emulsion polymerization. The conversion of MMA increased rapidly to 75.3% in 20 minutes and then gradually reached 89.7% in the next 20 minutes with the differential microemulsion polymerization, while it took 40 minutes for the soap-free emulsion polymerization to yield a monomer conversion of 61.2%. This could mainly be ascribed to the fact that in the differential polymerization, the initial polymerized microemulsion is abundant in the micelles of surfactant and therefore provides considerable particle nuclei. Meanwhile, the particles were much smaller in the microemulsion, which grants higher specific surface area to boost the diffusion of monomer to the burgeoning polymer particles.

The contrast in the size of polymer particles is depicted in Figure 11. There is a striking difference in the particle diameter from these two methods. The particles obtained by the soap-free emulsion polymerization were of hundreds of nanometers, whereas the differential microemulsion polymerization generated polymer particles of only tens of nanometers. The tendency of diameter versus residence time is also quite different. The average diameter in the soap-free emulsion increased gradually from 257 ± 36 nm to 515 ± 33 nm with the residence time from 12 min to 40 min. In the differential microemulsion polymerization, however, the average diameter of polymer particles underwent a slight decrease from 26.8 ± 4.9 nm to 12.0 ± 3.5 nm. From Figure 12, we can also observe that the size distributions of

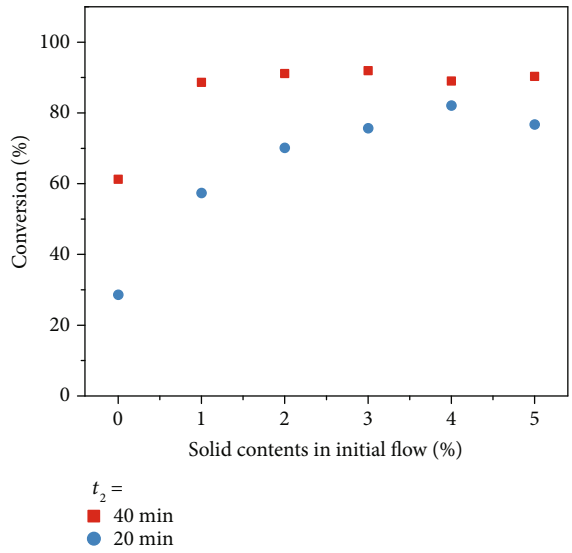

Figure 9: Effect of the solid content in the initial microemulsion on the monomer conversion (W : O = 1.5 : 1, $T = 80^{\circ}C$, $t_1 = 20$ min, and the concentration of APS was 5 mM).

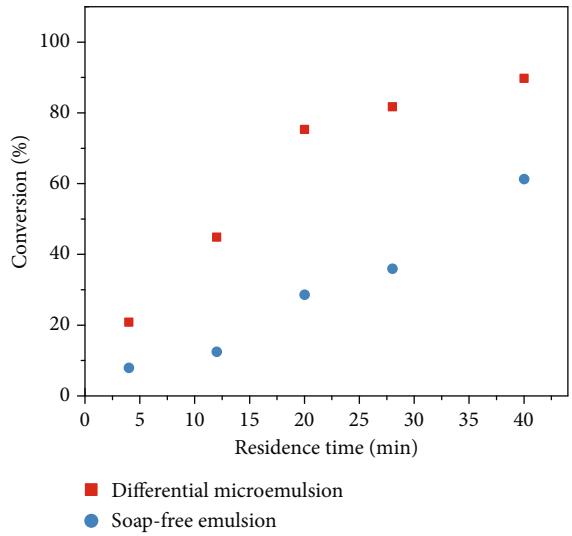

Figure 10: Conversion versus residence time profiles for differential microemulsion polymerization and soap-free emulsion polymerization (W : O = 1.5 : 1, $t_1 = 20$ min, $T = 80^{\circ}C$, the concentration of APS was 5 mM, and the solid content of the initial microemulsion was 5.0 wt.%).

these two methods evolved in different directions. The specific morphologies of the final latices prepared through these two methods were verified by SEM (see Figures S2–S5 in Supporting Information).

In the soap-free emulsion polymerization, the gradual increase in the particle diameter and the movement of the size distribution to the region of larger sizes all suggested that the polymer particles grew as more and more monomer molecules participated in the propagation. This supports that the particle nucleation mainly happened at one stage

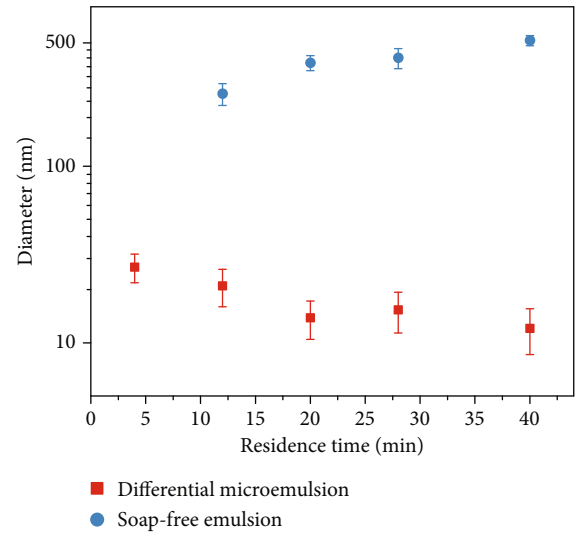

Figure 11: Number-average diameter of the latex particles versus residence time profiles for differential microemulsion polymerization and soap-free emulsion polymerization.

(*i.e.*, the aforementioned interval I) and the polymerization that follows took place within the particle nuclei. The case was not the same in the differential microemulsion polymerization. First, the particle nucleation occurred over most of the microemulsion polymerization, which is demonstrated in the kinetic study of microemulsion polymerization. As reported by O'Donnell and Kaler [38], throughout the microemulsion polymerization, the monomer-swollen micelles will shrink in their size but increase in their number density. Moreover, the differential microemulsion polymerization can be considered as a successive series of microemulsion polymerization in which the monomer is gradually fed into the reaction mixture. Taking these premises into consideration, one can safely deduce that the shrinking micelles along the process can provide a great number of particle nuclei for the monomer diffusing from the organic phase, thus forming uniform but often smaller particles. This should be able to account for our observation that the size of the latices slightly declined when they were prepared in the differential microemulsion polymerization. This tendency is also in good agreement with the work of Wang et al. [7]. They observed a decrease of the particle size as they prolonged the addition time of monomer when conducting differential microemulsion polymerization of MMA in a batch reactor.

It is obvious that the introduction of the prepolymerized microemulsion plays a pivotal role in the preparation of nanosized polymer latices in microreactors. On one hand, the polymerization rate is enhanced due to the abundance of particle nuclei and higher specific surface area of the smaller particles. On the other hand, the mechanism that particle nucleation occurs throughout the process enables the practice of differential microemulsion polymerization to curb the size of the final products in a small region.

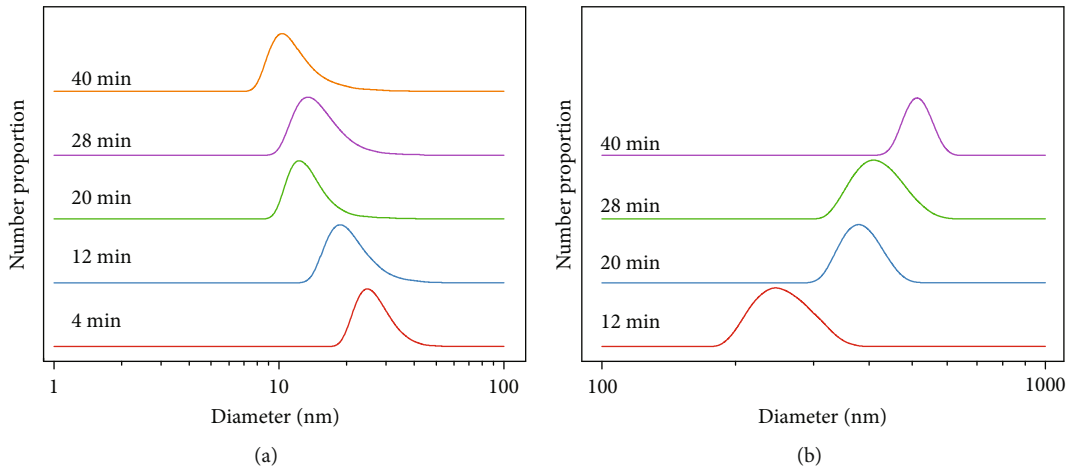

Figure 12: Evolution of particle size distribution in (a) differential microemulsion polymerization and (b) soap-free emulsion polymerization.

4. Conclusion

In this work, rapid and stable preparation of nanosized PMMA latices was realized by differential microemulsion polymerization in a continuous-flow microreactor with the biphasic slug flow.

Firstly, we studied the temperature thresholds under thermal and redox initiation, the effect of initiator concentration, and the kinetics of microemulsion polymerization in the microreactor. Redox initiators could help expand the envelope of polymerization temperature, and a higher amount of initiator was beneficial to effective initiation of polymerization. The kinetic study was done with a piecewise model as the rate of polymerization decreased dramatically when the polymerization was close to its completion. Meanwhile, this also demonstrated the mechanism that the particle nucleation exists in the whole microemulsion polymerization, which would only happen in the first stage of typical emulsion polymerization.

Next, the effects of the volumetric flow ratio, the prepolymerization time, the initiator concentration, and the solid content in the initial microemulsion were extensively examined. A higher volumetric flow ratio of the aqueous phase to the organic phase and a longer prepolymerization time all turned out to be helpful to boost the rate of polymerization. Meanwhile, latices could be prepared with a comparably high polymeric content (15.7%) in 20 min. The initiator concentration functioned in adjusting not only the rate of initiation and polymerization but also the molar mass properties of the final polymer products. Owing to the feature of emulsion polymerization, an impressive high number-average molecular weight (≥85 kg/mol) could be achieved even when a considerable amount of APS was used. Initial microemulsion with a higher solid content was capable to provide more micelles, thus improving the polymerization rate.

When there was only initiator in the aqueous phase, the soap-free emulsion polymerization was being carried out. Compared with the soap-free emulsion polymerization, the differential microemulsion polymerization displayed a much faster polymerization rate thanks to plenty of particle nuclei in the microemulsion and the higher specific surface area with smaller polymeric particles. The mechanism of the persistent particle nucleation in the microemulsion polymerization also allowed the production of PMMA latices whose particle size is smaller than 20 nm as more and more monomer was fed into the system.

Throughout this work, the strategy of differential microemulsion polymerization in microreactors within the biphasic slug flow has exhibited high reliability (no fouling was observed in the microreactor), high efficiency (e.g., a large polymeric content was quickly achieved), and most of all, the capability for rapid and steady preparation of fine polymer nanoparticles.

Data Availability

The characterization data used to support the results and discussion are available from the corresponding author upon request.

Conflicts of Interest

There are no conflicts to declare.

Acknowledgments

We would like to acknowledge the financial support from the National Natural Science Foundation of China (Nos. 92034303 and 21676164) and the Science and Technology Commission of Shanghai Municipality (No. 18520743500).

Supplementary Materials

The supporting information includes the pictures of polymer latices prepared with the initial microemulsion of different solid contents (Figure S1) and the morphology of polymer nanoparticles prepared by soap-free emulsion polymerization and differential microemulsion polymerization (Figures S2–S5). *(Supplementary Materials)*

References

[1] G. G. Odian, *Principles of Polymerization*, Wiley-Interscience, Hoboken, N. J, 4th ed edition, 2004.

[2] R. J. Young and P. A. Lovell, *Introduction to Polymers*, CRC Press, Boca Raton, 3rd ed edition, 2011.

[3] C. S. Chern, "Emulsion polymerization mechanisms and kinetics," *Progress in Polymer Science*, vol. 31, no. 5, pp. 443–486, 2006.

[4] A. Czajka and S. P. Armes, "Time-resolved small-angle X-ray scattering studies during aqueous emulsion polymerization," *Journal of the American Chemical Society*, vol. 143, no. 3, pp. 1474–1484, 2021.

[5] W. Ming, F. N. Jones, and S. Fu, "High solids-content nanosize polymer latexes made by microemulsion polymerization," *Macromolecular Chemistry and Physics*, vol. 199, no. 6, pp. 1075–1079, 1998.

[6] G. He, Q. Pan, and G. L. Rempel, "Synthesis of poly(methyl methacrylate) nanosize particles by differential microemulsion polymerization," *Macromolecular Rapid Communications*, vol. 24, no. 9, pp. 585–588, 2003.

[7] H. Wang, Q. Pan, and G. L. Rempel, "Micellar nucleation differential microemulsion polymerization," *European Polymer Journal*, vol. 47, no. 5, pp. 973–980, 2011.

[8] K. Wang, Y. C. Lu, J. H. Xu, X. C. Gong, and G. S. Luo, "Reducing side product by enhancing mass-transfer rate," *AICHE Journal*, vol. 52, no. 12, pp. 4207–4213, 2006.

[9] M. Movsisyan, E. I. P. Delbeke, J. K. E. T. Berton, C. Battilocchio, S. V. Ley, and C. V. Stevens, "Taming hazardous chemistry by continuous flow technology," *Chemical Society Reviews*, vol. 45, no. 18, pp. 4892–4928, 2016.

[10] J. Yoshida, A. Nagaki, and T. Yamada, "Flash chemistry: fast chemical synthesis by using microreactors," *Chemistry - A European Journal*, vol. 14, no. 25, pp. 7450–7459, 2008.

[11] J. Yoshida, H. Kim, and A. Nagaki, ""Impossible" chemistries based on flow and micro," *Journal of Flow Chemistry*, vol. 7, no. 3–4, pp. 60–64, 2017.

[12] T. Iwasaki and J. Yoshida, "Free radical polymerization in Microreactors. Significant Improvement in Molecular Weight Distribution Control," *Significant Improvement in Molecular Weight Distribution Control, Macromolecules*, vol. 38, no. 4, pp. 1159–1163, 2005.

[13] B. Wenn and T. Junkers, "Continuous microflow photoRAFT polymerization," *Macromolecules*, vol. 49, no. 18, pp. 6888–6895, 2016.

[14] W. Huang, J. Zhai, X. Hu et al., "Continuous flow photoinduced phenothiazine derivatives catalyzed atom transfer radical polymerization," *European Polymer Journal*, vol. 126, article 109565, 2020.

[15] A. Nagaki, K. Kawamura, S. Suga, T. Ando, M. Sawamoto, and J. Yoshida, "Cation pool-initiated controlled/living polymerization using microsystems," *Journal of the American Chemical Society*, vol. 126, no. 45, pp. 14702-14703, 2004.

[16] A. Nagaki, Y. Tomida, A. Miyazaki, and J. Yoshida, "Microflow system controlled anionic polymerization of alkyl methacrylates," *Macromolecules*, vol. 42, no. 13, pp. 4384–4387, 2009.

[17] Y. Liu, N. Zhu, X. Hu et al., "Continuous flow rare earth phenolates catalyzed chemoselective ring-opening polymerization," *Chemical Engineering Science*, vol. 211, article 115290, 2020.

[18] T. Iwasaki, N. Kawano, and J. Yoshida, "Radical polymerization using microflow system: numbering-up of microreactors and continuous operation," *Organic Process Research and Development*, vol. 10, no. 6, pp. 1126–1131, 2006.

[19] M. Qiu, L. Zha, Y. Song, L. Xiang, and Y. Su, "Numbering-up of capillary microreactors for homogeneous processes and its application in free radical polymerization," *Reaction Chemistry & Engineering*, vol. 4, no. 2, pp. 351–361, 2019.

[20] W. Huang, N. Zhu, Y. Liu et al., "A novel microfluidic enzyme-organocatalysis combination strategy for ring- opening copolymerizations of lactone, lactide and cyclic carbonate," *Chemical Engineering Journal*, vol. 356, pp. 592–597, 2019.

[21] J. H. Vrijsen, C. Osiro Medeiros, J. Gruber, and T. Junkers, "Continuous flow synthesis of core cross-linked star polymersviaphoto-induced copper mediated polymerization," *Polymer Chemistry*, vol. 10, no. 13, pp. 1591–1598, 2019.

[22] L. Xiang, M. Qiu, M. Shang, and Y. Su, "Continuous synthesis of star polymers with RAFT polymerization in cascade microreactor systems," *Polymer*, vol. 222, article 123669, 2021.

[23] Y. Song, J. Song, M. Shang et al., "Hydrodynamics and mass transfer performance during the chemical oxidative polymerization of aniline in microreactors," *Chemical Engineering Journal*, vol. 353, pp. 769–780, 2018.

[24] T. Watanabe, K. Karita, K. Tawara, T. Soga, and T. Ono, "Rapid synthesis of poly(methyl methacrylate) particles with high molecular weight by soap-free emulsion polymerization using water-in-oil slug flow," *Macromolecular Chemistry and Physics*, vol. 220, article 1900021, 2019.

[25] E. Lobry, F. Jasinski, M. Penconi et al., "Continuous-flow synthesis of polymer nanoparticles in a microreactor via miniemulsion photopolymerization," *RSC Advances*, vol. 4, no. 82, pp. 43756–43759, 2014.

[26] E. Lobry, F. Jasinski, M. Penconi et al., "Synthesis of acrylic latex via microflow miniemulsion photopolymerization using fluorescent and LED UV lamps," *Green Processing and Synthesis*, vol. 3, no. 5, pp. 335–344, 2014.

[27] X. Liu, Y. Lu, and G. Luo, "Continuous flow synthesis of polystyrene nanoparticles via emulsion polymerization stabilized by a mixed nonionic and anionic emulsifier," *Industrial and Engineering Chemistry Research*, vol. 56, no. 34, pp. 9489–9495, 2017.

[28] A. Chemtob, A. Rannée, L. Chalan, D. Fischer, and S. Bistac, "Continuous flow reactor for miniemulsion chain photopolymerization: understanding plugging issue," *European Polymer Journal*, vol. 80, pp. 247–255, 2016.

[29] V. Daniloska, R. Tomovska, and J. M. Asua, "Designing tubular reactors to avoid clogging in high solids miniemulsion photopolymerization," *Chemical Engineering Journal*, vol. 222, pp. 136–141, 2013.

[30] N. Kohut-Svelko, R. Pirri, J. M. Asua, and J. R. Leiza, "Redox initiator systems for emulsion polymerization of acrylates," *Journal of Polymer Science Part A: Polymer Chemistry*, vol. 47, no. 11, pp. 2917–2927, 2009.

[31] J. D. Morgan, K. M. Lusvardi, and E. W. Kaler, "Kinetics and mechanism of microemulsion polymerization of hexyl methacrylate," *Macromolecules*, vol. 30, no. 7, pp. 1897–1905, 1997.

[32] J. O'Donnell and E. W. Kaler, "Microstructure, kinetics, and transport in oil-in-water microemulsion polymerizations," *Macromolecular Rapid Communications*, vol. 28, no. 14, pp. 1445–1454, 2007.

[33] G. Li, M. Shang, Y. Song, and Y. Su, "Characterization of liquid–liquid mass transfer performance in a capillary microreactor system," *AIChE Journal*, vol. 64, no. 3, pp. 1106–1116, 2018.

[34] Y. Zhao, G. Chen, and Q. Yuan, "Liquid–liquid two-phase mass transfer in the T-junction microchannels," *AIChE Journal*, vol. 53, no. 12, pp. 3042–3053, 2007.

[35] J. C. Crittenden, R. R. Trussell, D. W. Hand, K. J. Howe, and G. Tchobanoglous, "Appendix C: Physical Properties of Water," in *MWH's Water Treatment: Principles and Design, Third Edition: Principles and Design, Third Edition*, pp. 1861-1862, John Wiley & Sons, Ltd, 2012.

[36] W. Fan, Q. Zhou, J. Sun, and S. Zhang, "Density, excess molar volume, and viscosity for the methyl methacrylate +1-butyl-3-methylimidazolium hexafluorophosphate ionic liquid binary system at atmospheric pressure," *Journal of Chemical & Engineering Data*, vol. 54, no. 8, pp. 2307–2311, 2009.

[37] Y. Liu, R. DiFoggio, K. Sanderlin, L. Perez, and J. Zhao, "Measurement of density and viscosity of dodecane and decane with a piezoelectric tuning fork over 298-448 K and 0.1-137.9 MPa," *Sensors and Actuators A: Physical*, vol. 167, no. 2, pp. 347–353, 2011.

[38] J. O'Donnell and E. W. Kaler, "Microstructure evolution and monomer partitioning in reversible addition–fragmentation chain transfer microemulsion polymerization," *Macromolecules*, vol. 41, no. 16, pp. 6094–6099, 2008.